ROTATIONAL HYSTERESIS OF Co FINE PARTICLES IN Cu—1%Co ALLOY

By J. M. Mucha*, L. Kozłowski and E. A. Japa

Department of Solid State Physics, Institute of Metallurgy, Academy of Mining and Metallurgy, Cracow**

(Received June 6, 1977)

Using the torque magnetometer rotational hysteresis losses of Cu—1%Co alloy were measured for different ageing times. The interpretation basing on extended Stoner and Wohlfarth theory including both shape and magnetocrystalline anisotropies is given.

1. Introduction

Knowledge of the type and size of magnetic anisotropy of single-domain ferromagnetic particles is essential in investigating materials suitable for permanent magnets. Analysis of the torque curves measured in strong magnetic fields enables one to determine the values of the magnetic anisotropy constants but does not provide information on the manner of magnetization of small particles nor on their shape. Measurement of rotational hysteresis can provide much broader information [1–3].

Rotational hysteresis losses with coherent reversal magnetization of single-domain particles have been discussed in detail by Stoner and Wohlfarth [4].

For materials with high values of the anisotropy constant K, and low saturation magnetization I_s, the critical magnetic field in the process of coherent rotation is very large, whereas for the majority of materials used for permanent magnet reversal magnetization occurs at much lower fields [2–6] in curling, fanning or buckling processes. The type of reversal magnetization depends on the shape of the particle [7].

In the present paper an interpretation is given for rotational hysteresis for Cu—1%Co monocrystals, assuming the simultaneous occurence of crystal and shape anisotropies.

* Address: Instytut Fizyki UJ, Reymonta 4, 30-059 Kraków, Poland.

** Address: Zakład Fizyki Ciała Stałego, Instytut Metalurgii, Akademia Górniczo-Hutnicza, Al. Mickiewicza 30, 30-059 Kraków, Poland.

The McCurrie [8, 9] model was used to determine the obtained results. In this model the Co particles are assumed to be rotational ellipsoids, the principal axes of which coincide with the crystallographic directions [100], [010] and [001].

2. *Experimental*

The rotational hysteresis was measured for Cu—Co monocrystals containing 1.01 %Co. The spectrographic analysis of impurity contents gave: 1 ppm As, 1 ppm Si, 1 ppm Mg and 2 ppm Fe. Discs 5 mm in diameter and 1 mm in thickness were used in the measurements performed with a torsion anisometer. Discs were cut in such a way that their planes coincided with the (001) plane. The accuracy of orientation was ± 0.0175 radians. In order to obtain a uniform solution of Co in Cu matrix samples were sintered in an oven in a protective atmosphere of argon at a temperature of 1273 K for 4 hours and then cooled to room temperature in an oil bath. Standardized samples were aged at 873 K. After given periods of ageing, samples were quenched in water to room temperature. Rotational hysteresis was measured for samples aged for periods of 3, 6, 9, 16, 24, and 700 hours.

Rotational hysteresis was given by the field enclosed between torque curves obtained by rotating the electromagnet from 0 to 2π "to-the-right" and from 2π to 0 "to-the-left". A detailed description of the construction and principle of operation of this anisometer, and of the experimental procedure, are given elsewhere [10, 11]. Rotational hysteresis losses were measured for room and liquid nitrogen temperatures, i.e. 300 K and 77 K. The accuracy of measurement was 3%.

3. *Experimental results*

The results of measurements of rotational hysteresis for samples aged over various periods are presented in the form of plots of the hysteresis versus magnetic field strength. In Fig. 1 results are presented of measurements of losses at 300 K. It is seen that for samples aged for up to 16 hours, the dependence losses vs magnetic field strength features one maximum. For a sample aged for 24 hours maxima are seen at two values of the magnetic field, one at 1.43×10^4 A/m and the other at 11.94×10^4 A/m. At the temperature 77 K (Fig. 2) a peak at low field values occurs for the sample aged 6 hours while for the sample aged for 3 hours no changes of rotational hysteresis are seen at either temperatures. In Fig. 3 rotational hysteresis of a sample aged for 700 hours is presented. In this case no peak is seen at low fields and loss values at 77 K and 300 K are similar.

It is worth noting that loss values in the maxima occurring at stronger fields do not vary much on cooling of the sample from 300 K to 77 K while the peak intensity at low fields increases with cooling time. For example, it may be noticed that for a sample aged 24 hours the value of losses at the low-field maximum for 300 K is six times smaller than that for 77 K .

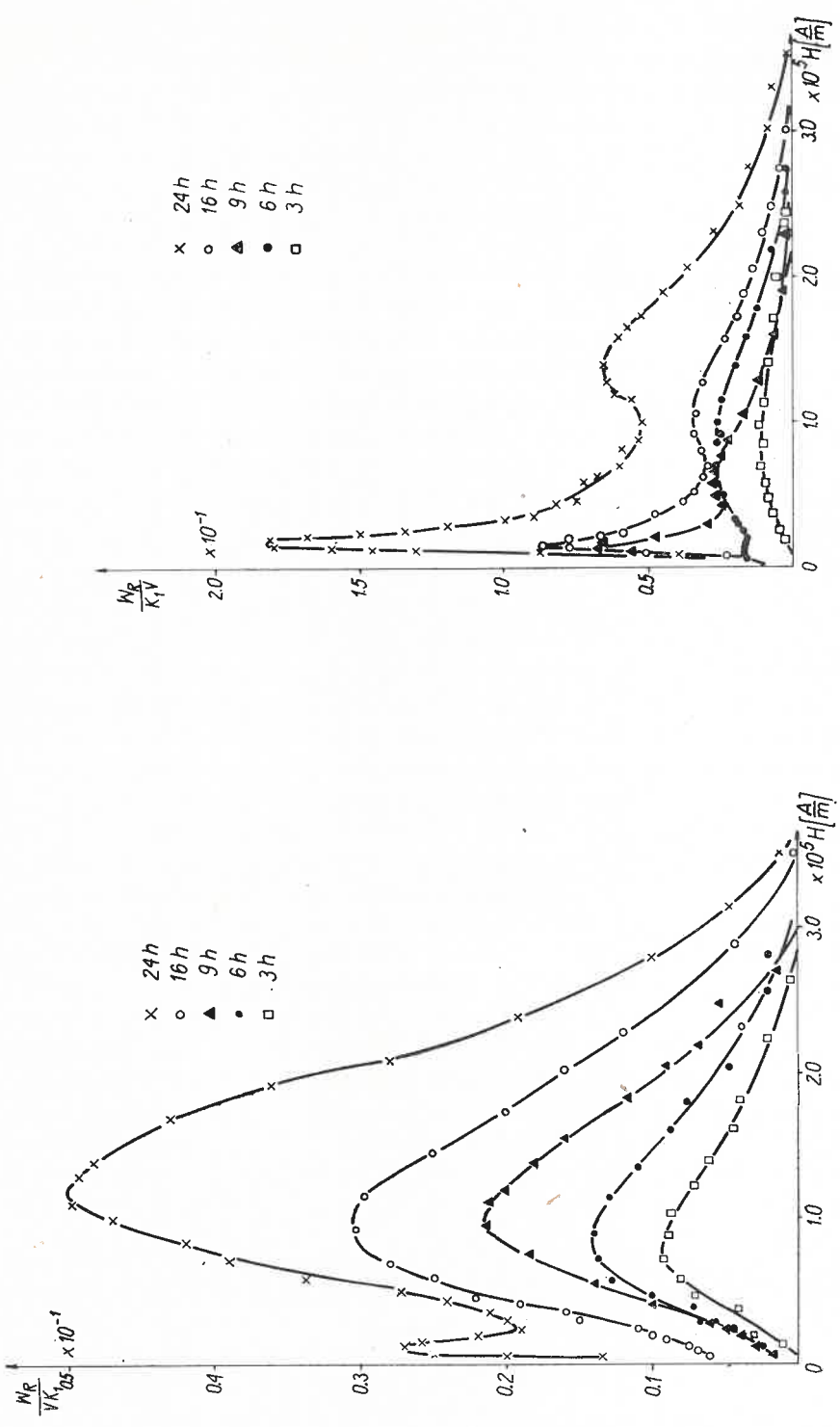

Fig. 1

Fig. 2

Fig. 1. Rotational hysteresis losses for differently aged samples, measured at 300 K
Fig. 2. Rotational hysteresis losses for differently aged samples, measured at 77 K

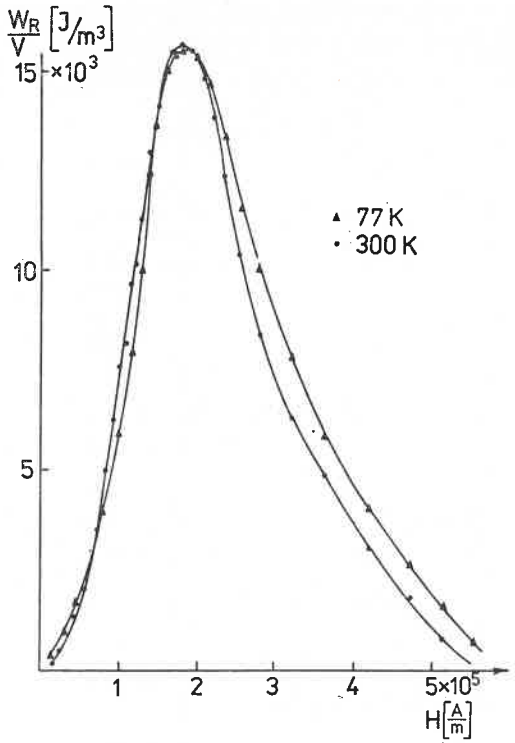

Fig. 3. Rotational hysteresis losses for a sample aged for 700 hours, at 300 K and 77 K

4. Theoretical considerations

4.1. Description of the model

The models of magnetization of single-domain particles discussed up to now do not explain the experimentally obtained behaviour of rotational hysteresis, even qualitatively. The assumption of various models [2–4] leads only to a widening of the lower range of fields in which losses of rotational hysteresis occur. To find an explanation, an analysis was carried out of critical fields for magnetization vector reversal by coherent rotation taking simultaneously into account crystal and shape anisotropies of a ferromagnetic particle. For this purpose it was assumed [9, 12] that small Co particles are of the shape of rotational ellipsoids the principal axes of which coincide with the [100], [010] and [001] directions. Under this assumption, in a disc-shaped sample in which the (001) monocrystal plane is parallel to the disc plane three groups of particles appear (Fig. 4). The first group consists of rotational ellipsoids the principal axes of which coincide with the [100] direction. The second group is formed of particles the main axes of which are parallel to the [010] direction, and the third group can be treated as spheres under rotations of the magnetization vector in the (001) plane. Critical fields for magnetization of this group are described by crystal anisotropy [13].

Introducing an additional assumption that all particles are of identical shape and that the energy of magnetostatic interaction of particles is small and can be neglected, the total energy of such a set of particles can be written in the following form:

$$E = E_1 + E_2 + E_3, \tag{1}$$

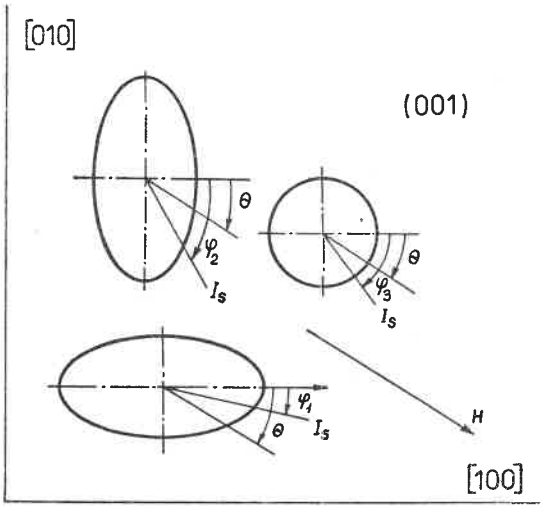

Fig. 4. Section of the Cu—Co monocrystal with the (001) plane

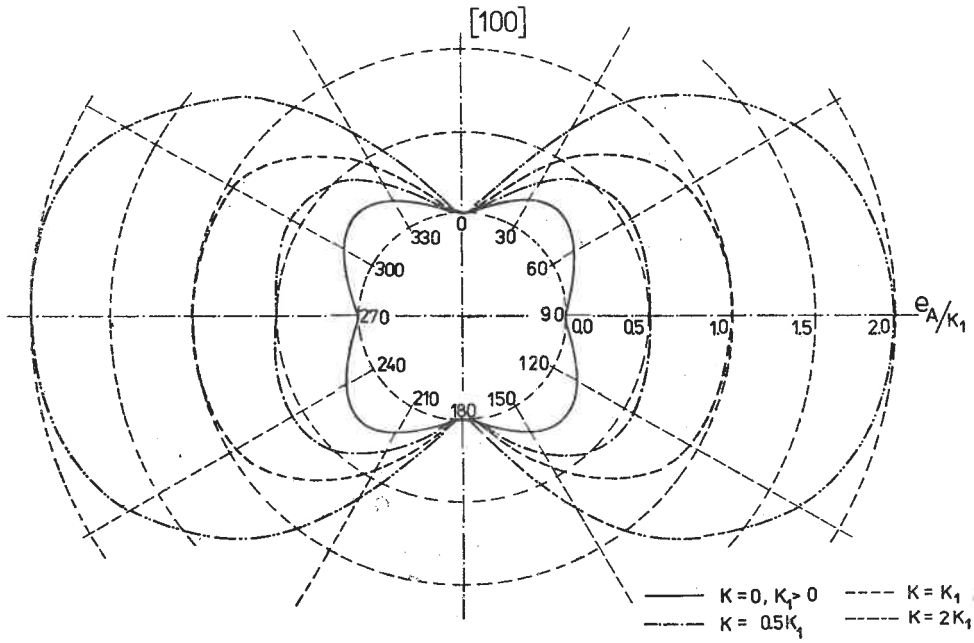

Fig. 5. Anisotropy energy of a particle with the shape of a rotational ellipsoid, the principal axis of which coincides with the [100] monocrystal direction, for various values K/K_1, $K_1 > 0$

where E_1, E_2, E_3 are the free energies of particles ellongated along the directions [100], [010] and [001], respectively. If the sample plane is the (001) monocrystal plane, then free energies of the given groups of particles are as follows:

$$E_1 = Kv_1 \sin^2 \varphi_1 + \frac{K_1 v_1}{4} \sin^2 2\varphi_1 - HI_s v_1 \cos(\theta - \varphi_1), \tag{2}$$

$$E_2 = Kv_2 \sin^2 (90^0 - \varphi_2) + \frac{K_1 v_2}{4} \sin^2 2\varphi_2 - HI_s v_2 \cos(\theta - \varphi_2), \tag{3}$$

$$E_3 = \frac{K_1 v_3}{4} \sin^2 2\varphi_3 - HI_s v_3 \cos(\theta - \varphi_3). \tag{4}$$

The angles φ_1 φ_2, φ_3 and θ are defined in Fig. 5. As none of the three crystallographic directions is preferred one may assume that

$$v_1 = v_2 = v_3 = \frac{V}{3}, \tag{5}$$

where V is the volume of the ferromagnet.

4.2. Anisotropy energy of particle

Let us study the case of a particle having the shape of a rotational ellipsoid, the principle axis of which coincides with the [100] monocrystal direction. The anisotropy energy density of such a particle is

$$e_A = K \sin^2 \varphi_1 + \frac{K_1}{4} \sin^2 2\varphi_1, \tag{6}$$

where e_A denotes the anisotropy energy density, K is the shape anisotropy constant and K_1 the crystal anisotropy constant. Extrema of the anisotropy energy occur at the position for which

$$\frac{de_A}{d\varphi_1} = K \sin 2\varphi_1 \left(1 + \frac{K_1}{K} \cos 2\varphi_1\right) = 0. \tag{7}$$

Analysing the sign of the second derivative of the expression giving the density of anisotropy energy for values which solve equation (7), one obtaines the following conditions:

— if $K_1 > 0$ and $K > K_1$ then the particle possesses one easy direction coinciding with the principal axis of the ellipsoid. The hard direction is perpendicular to the principal axis.

— if $K_1 > 0$ and $K < K_1$ then two directions appear along which the energy reaches minimum values. One of these directions coincides with the principal axis of the ellipsoid and the other form an angle $\pi/2$ with the principal axis. Hard directions occur at positions given by the relation

$$\cos 2\varphi_{1m} = -\frac{K}{K_1}, \tag{8}$$

where φ_{1m} is the angle between the hard directions and the axis of the particle (the principal particle axis coincides with the [100] monocrystal direction).

The dependence of energy on the angle for the case $K_1 > 0$ is shown in Fig. 5 for given values of the ratio K/K_1. As cubic cobalt has a negative constant of crystal anisotropy, this case will be discussed more extensivelly. If $K > -K_1$, then, as has been shown elsewhere (7), the easy particle direction coincides with the direction of the principal axis

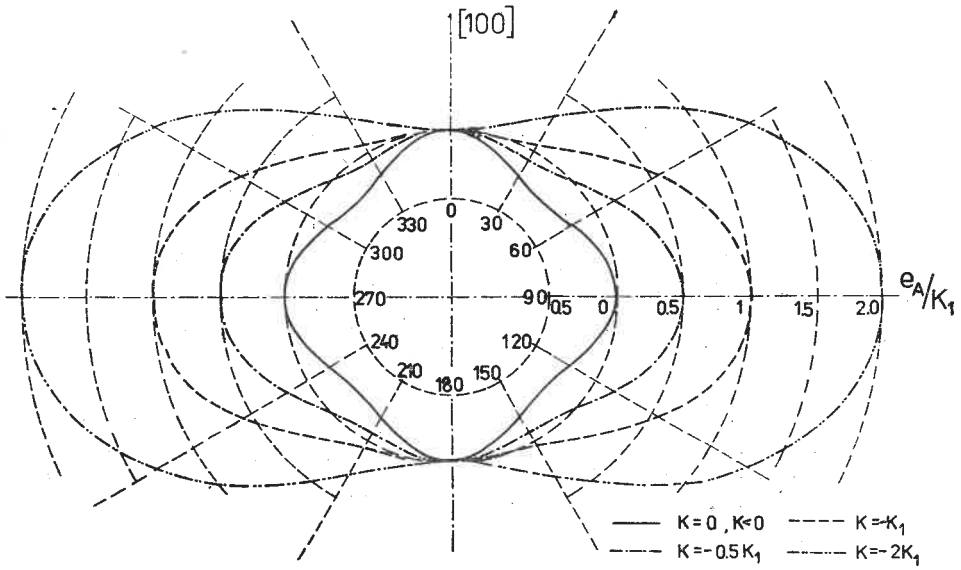

Fig. 6. Anisotropy energy of a particle with the shape a rotational ellipsoid the principal axis of which coincides with the [100] monocrystal direction, for various values K/K_1, $K_1 < 0$

and the hard direction is perpendicular to that axis. The energy of the particle behaves similarly to that for the case of particles of uniaxial anisotropy (Fig. 6). If $K < -K_1$ then the direction [100] (direction of the principal axis) ceases to be an easy direction. Easy directions occur at new positions. The angle between the easy direction and the direction [100] is given by the relation (8). As may be seen in the figure, a particle of this type possesses two minima, given by equation (8), and two maxima of anisotropy energy, each of different value. One of these maxima coincides with the [100] direction (along the principal axis of the ellipsoid), and the other with the [010] direction (perpendicular to that axis).

The values of energy barriers change, depending on the value of the ratio K/K_1. The value of the energy barier separating the two easy directions, φ_{1m} and $360° - \varphi_{1m}$ calculated from equation (6) is

$$\Delta e_{AI} = -\frac{K_1}{4}\left(1+\frac{K}{K_1}\right)^2, \tag{9}$$

and the value of the energy barrier separating the two neighbouring easy directions, φ_{1m}, and $180° - \varphi_{1m}$, is

$$\Delta e_{AII} = -\frac{K_1}{4}\left(1 - \frac{K}{K_1}\right)^2. \tag{10}$$

In Fig. 6 the angular dependence of anisotropy energy of a particle for which $K_1 < 0$ is shown for several values of the ratio K/K_1. The dependence for the special case, $K/K_1 = -0.5$, is shown separately in Fig. 7.

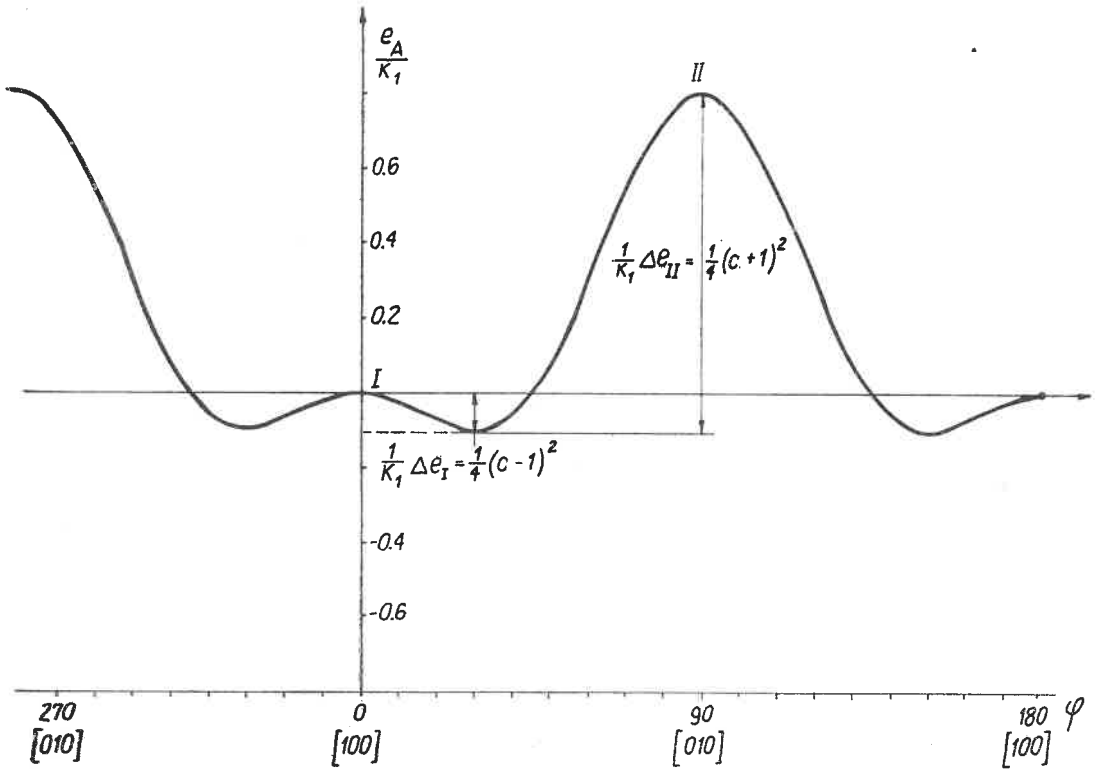

Fig. 7. Anisotropy energy vs angle measured from the principal axis of the particle, for the case when axis coincides with the [100] direction of the monocrystal, for $K/K_1 = -0.5$ and $K_1 < 0$

4.3. Calculation of critical fields

When both anisotropies are present simultaneously, the calculation of the dependence between φ and θ, for given H, is carried out similarly to the case when only one type of anisotropy is taken into account [1, 4]. Consider particle ensemble with energy E_1 (elongated in the [100] direction). The condition for minimum energy is

$$\frac{\partial E_1}{\partial \varphi_1} = Kv_1 \sin 2\varphi_1 + \frac{K_1 v_1}{2} \sin 4\varphi_1 - HI_s v_1 \sin(\theta - \varphi_1) = 0. \tag{11}$$

Introducing the following parameters:

$$h_1 = -\frac{HI_s}{2K_1} \quad \text{and} \quad c = -\frac{K}{K_1}, \tag{12}$$

from equation (11) one obtains

$$-c \sin 2\varphi_1 + \tfrac{1}{2} \sin 4\varphi_1 + 2h_1 \sin(\theta - \varphi_1) = 0. \tag{13}$$

Irreversible jumps of the magnetization vector will occur at such values of θ and φ for which the condition of minimum energy is fulfilled together with the following condition:

$$\frac{\partial^2 E_1}{\partial \varphi_1^2} = -c \cos 2\varphi_1 + \cos 4\varphi_1 - h_1 \cos(\theta - \varphi_1) = 0. \tag{14}$$

From equations (13) and (14) it is possible to determine the value of θ and φ for which, for given h_1, an irreversible jump of the magnetization vector occurs. From the analysis of conditions of the solution of these equations the h_1 field ranges are obtained within which irreversible jumps of the magnetization vector occur. In this case one obtains two critical field ranges associated with jumps of the magnetization vector over two different barriers of particle energy (9), (10). One solution, which has a physical sense for $c < 1$, gives critical fields within which irreversible jumps of the magnetization vector over the lower energy barrier occur (maximum along the direction of the principal axis)

$$h'_{1p} = \left[\frac{-c^4 + 20c^2 + 8 - c^3(c^2+8)^{1/2} - 8c(c^2+8)^{1/2}}{128}\right]^{1/2} \tag{15}$$

$$h'_1 = 1 - c, \tag{16}$$

where h'_{1p} denotes the field at which jumps over the lower maximum begin, and h'_1 denotes the field at which jumps cease to occur. The second pair of solutions gives the field ranges at which irreversible jumps over the higher energy barrier occur

$$h_{1p} = \left[\frac{-c^4 + 20c^2 + 8 + c^3(c^2+8)^{1/2} + 8c(c^2+8)^{1/2}}{128}\right]^{1/2}, \tag{17}$$

$$h_1 = 1 + c. \tag{18}$$

The dependences (15) and (16), as well as (17) and (18) are presented graphically in Fig. 8. It follows from calculation that, for a given c, if the field is lower than that given by the formula (17) (curve *2* in Fig. 8) rotation of magnetization vector through a more difficult particle direction is not possible. The magnetization vector oscillates reversibly around the easy direction.

Irreversible jumps occur for fields in the range given by equation (17) and (18) (the surface contained between curves 2 and 1 in Fig. 8). For fields larger than h_1 given by equation (18) (curve 1 in Fig. 8), the state of particle saturation is achieved. If $c < 1$, then besides the described range of fields, corresponding to the behaviour of the magnetization vector at rotating through the higher energy barrier, another range appears given

by equation (15) and (16) (curves *3* and *4* in Fig. 8) which distinguishes the field range of the same type, corresponding to a rotation of the magnetization vector over the lower energy barrier. The ratios of the critical field at which irreversible jumps occur to the critical field at which they disappear, calculated using equations (15) and (16), and (17)

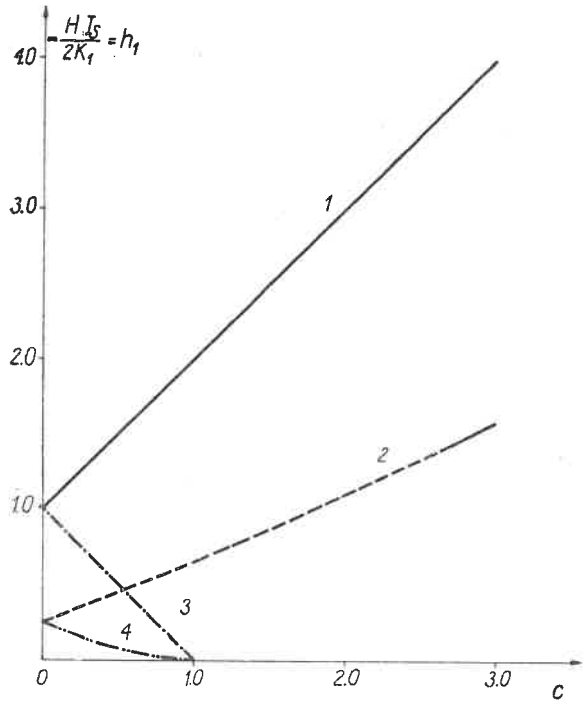

Fig. 8. Dependence h_{1p} and h_1 vs $c = -K/K_1$

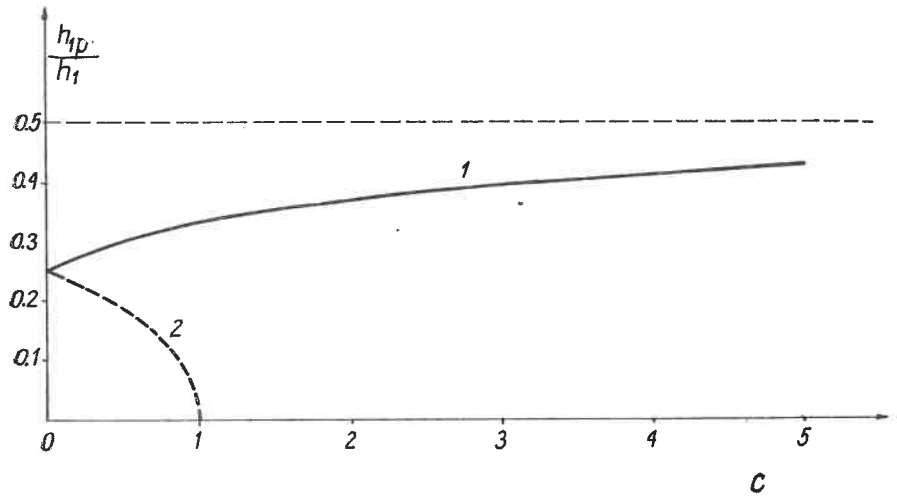

Fig. 9. Dependence of h_{1p}/h_1 vs $c = -K/K_1$

and (18), are shown in Fig. 9 as a function of c. $h_{1p}/h_1 = 0.25$ for $c = 0$ (crystal anisotropy of a cubic crystal) and approaches asymptotically the value $h_{1p}/h_1 = 0.5$ as $c \to \infty$ (curve *1* in Fig. 9), which corresponds to uniaxial anisotropy. Curve *2* in this figure shows the ratio h'_{1p}/h'_1. For $c = 0$ $h'_{1p}/h'_1 = 0.25$ and approaches zero for $c = 1$.

According to the above discussion and plots (Fig. 8) one concludes that in the case of such a particle, two types of irreversible jumps of magnetization vector are possible. Moreover one observes that for $c < 1$ two field range exist in which rotational hysteresis occur. If the value of the parameter c is smaller than about 0.55, then the critical field ranges for jumps over the high and low maxima energy partly overlap. For c values in the range $0.5 < c < 1$ one obtains two separate ranges. In the latter case rotational hysteresis appear for two field ranges. For $c > 1$ losses are of the same character as those for a particle with uniaxial anisotropy, but in this case the irreversible jumps of magnetization vector occur in the field range given by inequality $h_{1p} \leqslant h < h_1$. The critical fields and rotational hysteresis losses of [010] elongated particles are the same as those of the above discussed particles elongated along the [100] direction. Rotational hysteresis and critical field for the third group of particles, namely for those elongated along the [001] direction, are the same as those for a regular crystal, i.e. losses occur for field equal to $H = -0.25$ $2K_1/I_s$ and disappear for $H = -2K_1/I_s$.

5. *Interpretation of the experimental results*

From the earlier discussion in § 4 it follows that the behaviour of rotational hysteresis losses as a function of magnetic field intensity depends on the value of the ratio between the constants of shape and crystal anisotropies, K/K_1. Depending on the value of this ratio, one or two maxima may appear in the curve. Fields at which these maxima occur are associated with the value of the ratio K/K_1 through equations (15), (16) and (17), (18). Thus, a simple model enables one to explain the observed behaviour of rotational hysteresis obtained experimentally for the Cu – 1 %Co alloy. It may be seen in Fig. 1 and Fig. 2 that the positions of the maxima of losses in weak magnetic fields do not change much with ageing times. A more detailed calculation was performed for a sample aged for 24 hours. For this sample the first maximum occurs at the field $H = 1.27 \times 10^4$ A/m. To perform calculations values of the crystal anisotropy constant for samples aged for various periods were taken from literature [14, 15]. The reduced field $h = -HI_s/2K_1$ corresponding to the maximum calculated using the above data is $h = 0.089$. It is seen from the plot in Fig. 8 that for such h values only rotational hysteresis connected with irreversible jumps of the magnetization vector through the lower barrier energy (given by Eq. (10)) are possible. The value of the ratio $c = -K/K_1$ corresponding to this critical field, determined using the plot in Fig. 8, is equal to $c = 0.5$. The reduced field h at which rotational hysteresis over the lower energy barrier disappear at that c value (Eq. (16)) is $h = 0.5$, which corresponds to $H = 7.22 \times 10^4$ A/m.

From the discussion presented in § 4 it follows that such particles have a second, higher energy barrier. Irreversible jumps of the magnetization vector over that barrier begin for the field $H = 6.35 \times 10^4$ A/m and end for $H = 21.7 \times 10^4$ A/m. If only crystal

anisotropy is included, losses should begin to appear at $H = 4.82 \times 10^4$ A/m and cease at $H = 14.48 \times 10^4$ A/m. The model discussed in § 4 enables one to explain the appearance of rotational hysteresis in magnetic fields lower than those expected for a regular crystal without accounting for particle shape anisotropy.

At this stage quantitative interpretation is rather difficult, owing to the fact that this maximum would arise from losses connected with irreversible jumps of the magnetization vector over the barrier of anisotropy energy of particles of with non-zero values of the shape anisotropy coefficient K, as well as from spherically shaped particles.

TABLE I

Field intensities H_m at which strong-field maxima occur, fields H_d at which rotational hysteresis losses disappear and values of $c = -K/K_1$ calculated from torque measurements [14] and from field values H_m and H_d. The H_m and H_d values were obtained from rotational hysteresis measurements

A) Room temperature (300 K)

Ageing time [hour]	H_m [A/m] $\times 10^{-4}$	H_d [A/m] $\times 10^{-4}$	$-K_1$* [J/m^3] $\times 10^{-4}$	K* [J/m^3/] $\times 10^{-4}$	$-2K_1$*/I_s [A/m] $\times 10^{-4}$	c*	c calcul. from H_m	c calcul. from H_d
1	2	3	4	5	6	7	8	9
3	7.56	27.06	9.02	2.65	11.39	0.30	1.02	1.35
6	8.70	30.24	9.20	3.50	11.62	0.38	1.24	1.60
9	9.55	29.84	9.35	4.35	11.81	0.46	1.37	1.52
16	9.95	34.76	9.72	6.35	12.35	0.57	1.40	1.83
24	11.94	36.60	10.17	8.45	12.84	0.83	1.60	1.85
700 [a]	11.51	58.09	—	—	13.65	—	2.38	3.25

B) Liquid nitrogen temperature (77 K)

1	2	3	4	5	6	7	8	9
3	7.96	27.85	10.10	2.65	12.78	0.26	0.94	1.17
6	7.96	29.44	10.32	3.50	13.03	0.34	0.89	1.25
9	5.41	21.88	10.50	4.35	13.26	0.41	0.41	0.65
16	10.47	35.81	10.90	6.35	13.83	0.57	1.30	1.58
24	13.43	36.31	11.41	8.45	14.48	0.74	1.70	1.52
700 [a]	18.30	62.47	—	—	15.41	—	2.07	3.05

* K_1, K and c values obtained from the analysis of torque curves [14].
[a] K_1 values taken from extrapolation corresponding to solid material.

The observed large increase in losses observed while cooling the samples aged for 24 hours from 300 K to 77 K can only be explained by the increase in the number of stable particles. The position of the peak, close to that expected theoretically for cubic crystals, proves that small-sized particles have a roughly spherical shape (at 300 K they are superparamagnetic and give no rotational hysteresis [16], and at 77 K they become stable).

For all samples there appears a broad maximum at stronger fields. Fields for which the second maximum in the loss curves appears and fields at which these losses disappear are listed in Table I. In those tables also c values determined from the analysis of torque curves, taken from [14] are listed. It is seen from this Table that c values determined at 77 K are lower than those obtained for 300 K. These results confirm other investigations [14] where it was found that K_1 can change with temperature while K is the same for both temperatures. Also, c values determined from the second peak are larger than those determined from the torque curves. Moreover, for the sample aged for 24 hours, the c value determined from the second maximum differs considerably from the respective value found from the low field peak. The latter value is closer to that obtained from the analysis of the torque curves. This is connected with the fact that rotational hysteresis does not "see" superparamagnetic particles [16] whereas such particles contribute to the torque curve.

6. Concluding remarks

In conclusion, one should stress that the magnetic properties of small particles of the Cu – 1 %Co alloy cannot be described by taking into account only crystal anisotropy or only shape anisotropy. It is necessary to include both factors simultaneously.

The six-fold increase of the low field peak observed on cooling the sample aged for 24 hours from 300 K to 77 K, or the appearance of this peak in samples aged for shorter periods, can only be explained by the increase in the number of stable particles during cooling. It follows that this peak is due to small-sized particles which at 300 K are superparamagnetic and do not contribute to rotational hysteresis and which at 77 K become stable and then contribute. Because the range of fields for which the low field peak appears is close to field values for which rotational hysteresis losses occur for cubic crystals, it follows that small-size particles have almost spherical shapes (have low values of the shape anisotropy constant) and thus a low value of c. Small differences between rotational hysteresis for high magnetic fields at 300 K and 77 K would indicate that these arise from particles stable at both temperatures. Moreover, very small differences between the positions of maxima and between the field values at which these peaks disappear, indicate that shape anisotropy dominates. As was shown elsewhere [14], this anisotropy does not change with temperature.

One concludes that the model of McCurrie assumed here comprising both crystal and shape anisotropies, is too simple to explain the obtained experimental results. It seems that in order to achieve quantitative agreement, one would have to include, on the one hand, the fact that particles exhibit a distribution of shape anisotropies including at the same time the distribution of particle volumes, and on the other hand, one should also take into account the fact that particles of dimensions smaller than a critical dimension are superparamagnetic and do not exhibit rotational hysteresis. However, such an approach is difficult for mathematical reasons. Despite this, one can conclude that the results obtained from analysis of rotational hysteresis do not contradict the assumed model of uniform rotation which takes into account both types of anisotropy.

REFERENCES

[1] K. Schüller, *Z. Metallk.* **52**, 492 (1961).
[2] E. H. Frei, S. Shtrikman, D. Treves, *Phys. Rev.* **106**, 446 (1957).
[3] I. S. Jacobs, C. P. Bean, *Phys. Rev.* **100**, 1060 (1955).
[4] E. C. Stoner, E. P. Wohlfarth, *Phil. Trans. Roy. Soc.* **A240**, 599 (1948).
[5] A. Aharoni, *J. Appl. Phys.* **30**, *Suppl.* 70S (1959).
[6] F. E. Luborsky, *J. Appl. Phys.* **32**, *Suppl.* 171S (1961).
[7] W. F. Brown, Jr., *The Fundamental Theorems of the Theory of Fine Ferromagnetic Particles*, Publ. by Acad. N.Y. (1969).
[8] R. A. McCurrie, P. Gaunt, *Philos. Mag.* **19**, 339 (1969).
[9] R. A. McCurrie, *Philos. Mag.* **21**, 769 (1970).
[10] J. L. Majewski, E. A. Klus, J. M. Mucha, *Acta Phys. Pol.* **A44**, 671 (1973).
[11] E. A. Klus, J. M. Mucha, *Zeszyty Naukowe AGH* **331**, 57 (1973), (in Polish).
[12] M. Ernst, J. Schelten, W. Schmatz, *Phys. Status Solidi* (a) **7**, 477 (1971).
[13] J. M. Mucha, Thesis, AGH Cracow 1974 (in Polish).
[14] J. M. Mucha, L. Kozłowski, E. A. Japa, *Acta Phys. Pol.* **A50**, 149 (1976).
[15] H. Figiel, F. Ciura, J. Żukrowski, Materials of VII Electron Microscopy Conference, Berlin 1973.
[16] E. Köster, *J. Appl. Phys.* **41**, 3332 (1971).